

Scientific Research and Essays

Volume 11 Number 19 15 October, 2016

ISSN 1992-2248



ABOUT SRE

The Scientific Research and Essays (SRE) is published twice monthly (one volume per year) by Academic Journals.

Scientific Research and Essays (SRE) is an open access journal with the objective of publishing quality research articles in science, medicine, agriculture and engineering such as Nanotechnology, Climate Change and Global Warming, Air Pollution Management and Electronics etc. All papers published by SRE are blind peer reviewed.

Contact Us

Editorial Office: sre@academicjournals.org

Help Desk: helpdesk@academicjournals.org

Website: <http://www.academicjournals.org/journal/SRE>

Submit manuscript online <http://ms.academicjournals.me/>.

Editors

Dr. NJ Tonukari

*Editor-in-Chief
Scientific Research and Essays
Academic Journals
E-mail:sre.research.journal@gmail.com*

Dr. M. Sivakumar Ph.D. (Tech).

*Associate Professor
School of Chemical & Environmental Engineering
Faculty of Engineering
University of Nottingham
JalanBroga, 43500 Semenyih
SelangorDarul Ehsan Malaysia.*

Prof. N. Mohamed ElSawi Mahmoud

*Department of Biochemistry, Faculty of science, King
Abdul Aziz university,
Saudi Arabia.*

Prof. Ali Delice

*Science and Mathematics Education Department, Atatürk
Faculty of Education,
Marmara University, Turkey.*

Prof. Mira Grdisa

*RudjerBoskovicInstitute, Bijenicka cesta 54,
Croatia.*

Prof. Emmanuel HalaKwon-Ndung

*Nasarawa State University Keffi Nigeria
PMB1022 Keffi,
Nasarawa State.
Nigeria.*

Dr. Cyrus Azimi

*Department of Genetics, Cancer Research Center,
CancerInstitute, Tehran University of Medical Sciences,
Keshavarz Blvd.,
Tehran, Iran.*

Dr. Gomez, Nidia Noemi

*National University of San Luis,
Faculty of Chemistry, Biochemistry and Pharmacy,
Laboratory of Molecular Biochemistry
EjercitodelosAndes950-5700 SanLuis
Argentina.*

Prof.M.Nageeb Rashed

*Chemistry Department-Faculty of Science,
Aswan South Valley University,
Egypt.*

Dr. John W. Gichuki

*KenyaMarine& FisheriesResearchInstitute,
Kenya.*

Dr. Wong Leong Sing

*Department of Civil Engineering,
College of Engineering,
Universiti Tenaga Nasional,
Km7, JalanKajang-Puchong,
43009Kajang, SelangorDarulEhsan, Malaysia.*

Prof. Xianyi Li

*College of Mathematics and Computational Science
Shenzhen University Guangdong, 518060
P.R.China.*

Prof. Mevlut Dogan

*Kocatepe University, Science Faculty, Physics Dept.
Afyon/Turkey.
Turkey.*

Prof. Kwai-Lin Thong

*Microbiology Division, Institute of Biological Science,
Faculty of Science, University of Malaya, 50603,
KualaLumpur,
Malaysia.*

Prof. Xiaocong He

*Faculty of Mechanical and Electrical Engineering, Kunming
University of Science and Technology, 253 XueFu Road,
Kunming,
P.R.China.*

Prof. Sanjay Misra

*Department of Computer Engineering
School of Information and Communication Technology
Federal University of Technology, Minna,
Nigeria.*

Prof. Burtram C. Fielding Pr. Sci. Nat.

*Department of Medical BioSciences
University of the Western Cape Private Bag X17
Modderdam Road
Bellville, 7535, South Africa.*

Prof. Naqib Ullah Khan

*Department of Plant Breeding and Genetics
NWFP Agricultural University Peshawar 25130,
Pakistan*

Editorial Board

Prof. Ahmed M. Soliman

*20 Mansour Mohamed St., Apt 51, Zamalek,
Cairo,
Egypt.*

Prof. Juan José Kasper Zubillaga

*Av. Universidad 1953 Ed. 13 depto 304,
México D.F. 04340,
México.*

Prof. Chau Kwok-wing

*University of Queensland Instituto
Mexicanodel Petroleo, Eje Central
Lazaro Cardenas Mexico D.F.,
Mexico.*

Prof. Raj Senani

*Netaji Subhas Institute of Technology,
Azad Hind Fauj Marg, Sector 3,
Dwarka, New Delhi 110075, India.*

Prof. Robin J Law

*Cefas Burnham Laboratory,
Remembrance Avenue Burnhamon Crouch, Essex
CM08HA,
UK.*

Prof. V. Sundarapandian

*Indian Institute of Information Technology and
Management-Kerala
Park Centre,
Technopark Campus, Kariavattom P.O.,
Thiruvananthapuram-695581, Kerala, India.*

Prof. Tzung-Pei Hong

*Department of Electrical Engineering,
And at the Department of Computer Science and
Information Engineering
National University of Kaohsiung.*

Prof. Zulfiqar Ahmed

*Department of Earth Sciences, box 5070,
Kfupm, dhahran-31261, Saudi Arabia.*

Prof. Khalifa Saif Al-Jabri

*Department of Civil and Architectural Engineering
College of Engineering, Sultan
Qaboos University
P.O. Box 33, Al-Khod 123, Muscat.*

Prof. V. Sundarapandian

*Indian Institute of Information Technology &
Management-Kerala
Park Centre,
Technopark, Kariavattom P.O.
Thiruvananthapuram-
695581, Kerala India.*

Prof. Thangavelu Perianan

*Department of Mathematics,
Aditanar College,
Tiruchendur-628216 India.*

Prof. Yan-ze Peng

*Department of Mathematics,
Huazhong University of Science and
Technology, Wuhan 430074, P.R.
China.*

Prof. Konstantinos D. Karamanos

*Universite Libre de Bruxelles,
CP231 Centre of Nonlinear
Phenomena And Complex systems,
CENOLIB Boulevard de Triomphe
B-1050,
Brussels,
Belgium.*

Prof. Xianyi Li

*School of Mathematics and Physics,
Nanhua University, Hengyang City,
Hunan Province,
P.R. China.*

Dr. K.W. Chau

*Hong Kong Polytechnic University
Department of Civil & Structural
Engineering, Hong Kong Polytechnic
University, Hung Hom, Kowloon,
Hong Kong,
China.*

Dr. Amadou Gaye

*LPAO-SF/ESPPo Box 5085 Dakar-Fann SENEGAL
University Cheikh Anta Diop
Dakar SENEGAL.*

Prof. Masno Ginting

*P2F-LIPI, Puspiptek-Serpong,
15310 Indonesian Institute of Sciences,
Banten-Indonesia.*

Dr. Ezekiel Olukayode Idowu

*Department of Agricultural Economics,
Obafemi Awolowo University, Ife-Ife,
Nigeria.*

Scientific Research and Essays

Table of Contents: Volume 11 Number 19 15 October, 2016

ARTICLES

- Evaluation of reinforced concrete buildings in Northern Cyprus using TEC2007 and EC8 in respect of cost estimation** 194
A. Rifat Reşatoğlu and Rami S. Atiyah
- Dynamic modelling and predictive health monitoring for vibration control and resonance of rotating machinery** 202
A. Chellil, I. Gahlouz, S. Lecheb, S. Chellil, A. Nour and H. Mechakra

Full Length Research Paper

Evaluation of reinforced concrete buildings in Northern Cyprus using TEC2007 and EC8 in respect of cost estimation

Rifat Reşatoğlu^{1*} and Rami S. Atiyah²

¹Department of Civil Engineering, Faculty of Engineering, Near East University, Nicosia, North Cyprus.

²Technical Department, Ministry of Constructions and Housing, Baghdad, Iraq.

Received 16 August, 2016 Accepted 27 September, 2016

Cyprus lies in a seismic zone and the whole island (northern and southern part of the island) can be considered as an earthquake vulnerable area. In the last years, earthquake design of reinforced concrete structures becomes an important phenomenon due to unfortunate earthquakes. This amplifies the need to make such buildings earthquake resistant at a reasonably low cost. Most of the buildings are mid-rise reinforced concrete structures in two parts of the island. In this study, Turkish earthquake code 2007 (TEC2007) and Eurocode 8 (EC 8) design rules are examined and both regulations are compared for Northern Cyprus. Each design code use different seismic zoning maps with different peak ground acceleration values. These two regulations are compared with each other in terms of cost according to results of reinforced concrete structure in the range of three to seven storey ordinary apartment buildings, constructed in Nicosia.

Key words: TEC2007, EC8, Cyprus.

INTRODUCTION

Cyprus lies in one of the active seismic regions of the Eastern Mediterranean basin. The island was struck by numerous earthquakes in its history. The latest significant earthquake hit the island in 1953 with surface-wave magnitude of 6.5 and caused 40 fatalities (Ambrasey, 2009).

Devastating earthquakes hit all around the world and caused many deaths and injuries and left a lot of structures with substantial damage because of their weakness to withstand the earthquake events due to poor detailing of seismic resisting building according to inadequate design codes. Since then many seismic

codes were published in all around the world (Ersoy et al., 2000).

Currently two different design codes are used in Cyprus due to political issues. Turkish Earthquake Code 2007 (TEC2007) and Eurocode 8 (EC8) are used where the two code uses different seismic zone maps and different peak ground acceleration (PGA) values.

For Northern Cyprus (northern part of the island) currently, there is no detailed and official seismic zone map. The TEC2007 is being used and PGA values have been adopted to the code in the northern part of the island, having the PGA value of 0.3 g for Nicosia.

*Corresponding author. E-mail: rifat.resatoglu@neu.edu.tr.



Figure 1. Seismic Zoning Map of Cyprus from EC8 National Annex CY EN 1998-1:2004.

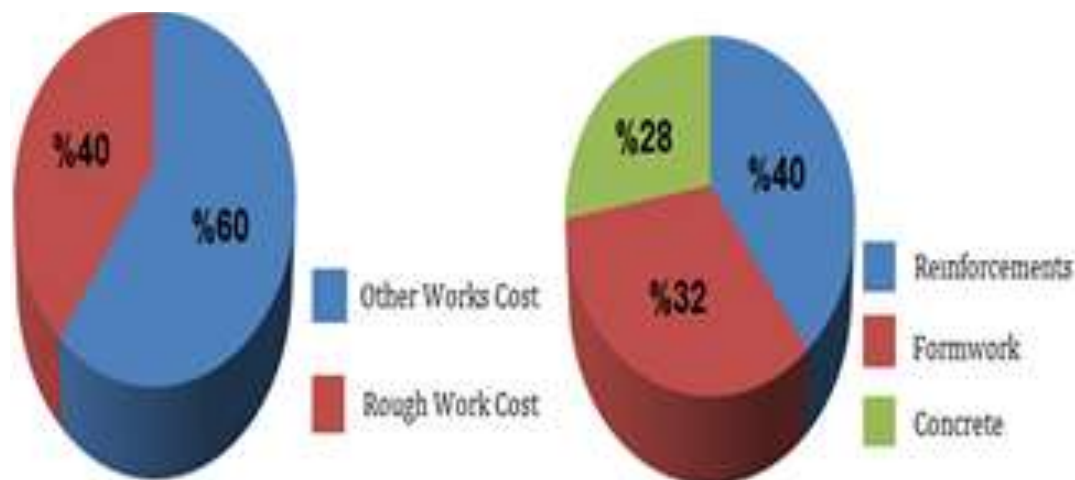


Figure 2. Typical distributions of reinforced concrete building construction costs.

EC8 Cyprus National Annex provided seismic zoning map of Cyprus having the PGA value of 0.2 g for Nicosia is shown in Figure 1 (CEN, 2004).

According to the TEC2007 where the seismic map has been adapted to the code in the northern part of the island, higher PGA values can be seen compare to the EC8 map. Both seismic maps have 10% exceedance probability in 50 years.

From 1960s till today, reinforced concrete structures are dominant building construction material in Northern and Southern Cyprus. The total construction cost for a new building is one of the most important aspect of building and a big concern for any owner. In general, rough constructions work in multi-storey reinforced concrete building corresponds to the approximately 40%

of the total cost of reinforced concrete building structure construction cost. This rough construction works consists of; reinforcement work, concrete work and formwork (Nunnally, 2007). Typical distributions of rough work construction costs for reinforced concrete building, in percentage are shown in Figure 2.

The rough construction of an ordinary apartment building which is chosen in this study can be seen in Picture 1.

MATERIALS AND METHODS

An ordinary apartment building, 3 to 7 storey has been chosen for the case study. Case study is chosen in Nicosia, which is Europe's last divided capital in Cyprus. General building information's of



Picture 1. Rough construction of an ordinary apartment building in Nicosia.

Table 1. General information of an ordinary apartment building in Nicosia.

Type of structure	Reinforced concrete
Storey height	3.00 m
Total floor area	238 m ²
Intended purpose	Residential
Concrete class	C25
Steel class	S420

these ordinary apartment buildings are shown in Table 1. Only one site location and one ordinary apartment building type has been used for the analysis. The investigated reinforced concrete frame building is designed as per the considered seismic codes and the corresponding design codes. The design codes are Eurocode 2 (EC2) (CEN, 2004) and TS500 (Turkish Standards Institute, 2000) respectively.

It is assumed that the investigated reinforced concrete building structures are established in Cyprus-Nicosia, where the ground conditions and seismic zone coefficient according to the national annex of this area are considered in the design.

During the analysis, foundations have been neglected. Therefore, only the superstructure has been analyzed. Load combinations were taken according to TEC2007 and EC8.

The plan dimensions of the investigated reinforced concrete building structure's, typical at all floors are, 15.4 m in the direction of X, and 16.8 m in the direction of Y, which is symmetric in one direction (Figure 3).

The dimension of beams, columns and slabs are given in Tables 2 to 4 respectively. The layout of shear-wall is given in Appendix Figure 1.

The analyzing and designing of the reinforced concrete buildings is made by using STA4-CAD V12.1 commercial computer program.

STA4-CAD is an integrated package program of software capable of executing three dimensional analyses (Figure 4).

The reinforced concrete building data are used as a program input data to design multi-storey buildings according to EC8 and TEC2007 rules and limitations.

In general there are two types of data used for the building's design which are general building datas and specific building datas.

The general building datas are common between EC8 and TEC2007 for the investigated buildings, as shown in Table 5.

Currently, all seismic design codes take into account the effect of inelastic energy dissipation by reducing the design seismic force by a response reduction factor also called behaviour factor. For the case study, high ductile design has been chosen for both codes. The provided ductility reduction factors are 5.85 and 8 for EC8 and TEC2007 respectively.

Specific data for reinforced concrete building design according to EC8

The specific data's for reinforced concrete building design according to EC8 which is used to design and analyze the buildings are shown in Table 6.

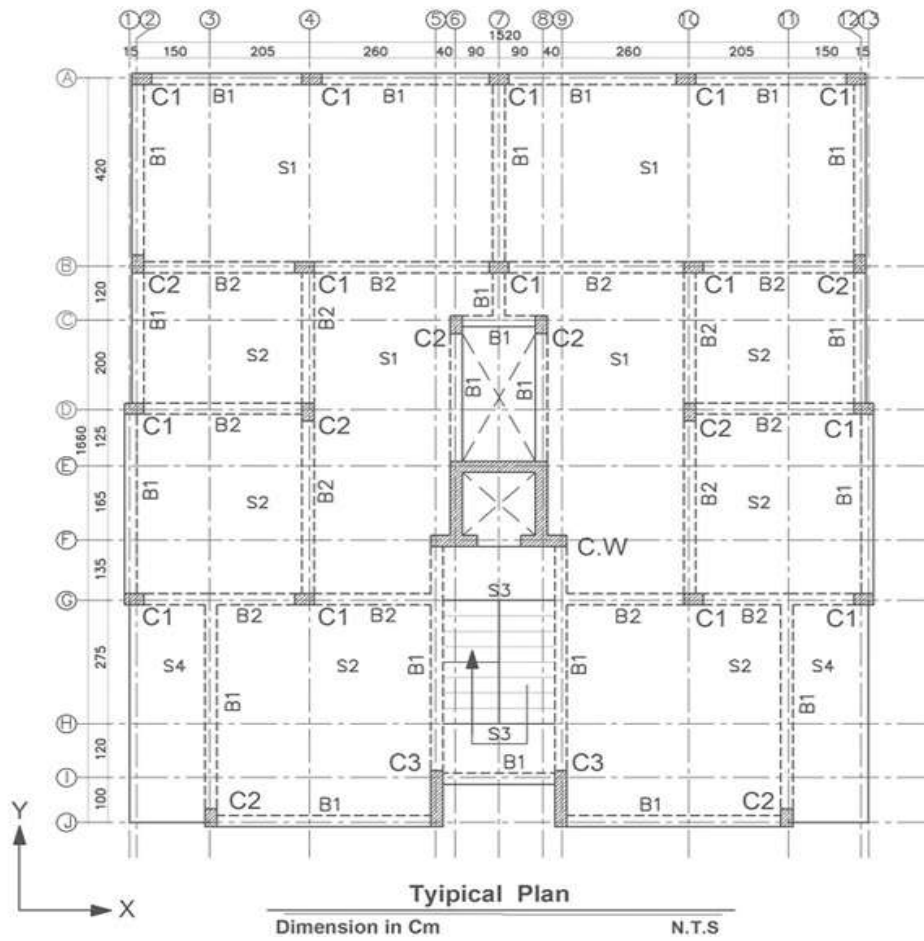


Figure 3. Typical plan of the investigated reinforced concrete building.

Table 2. Layout of beams for multi-storey reinforced concrete building.

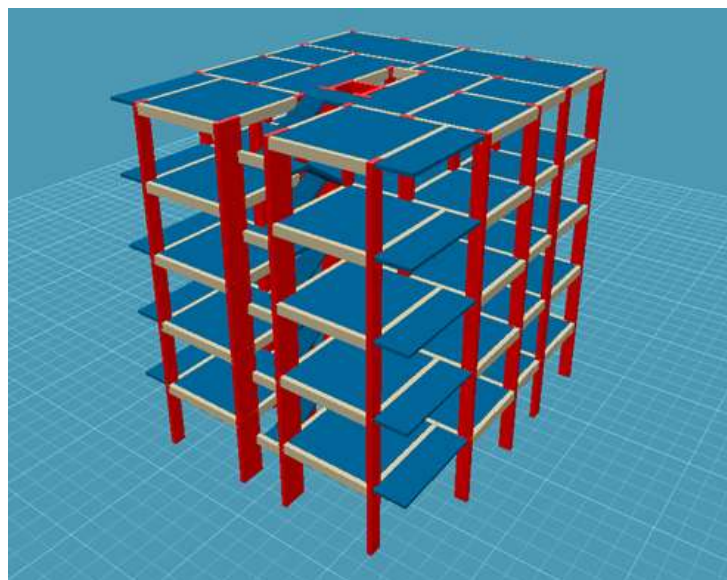
Number of storey	Beam type	Dimensions	Type of carrying wall
3, 4, 5, 6 and 7	B1	25 × 50	External walls
	B2	25 × 50	Internal walls

Table 3. Layout of columns for multi-storey reinforced concrete building.

Number of storey	Column type	b_x	b_y
3	C1	40	25
	C2	25	40
	C3	25	125
4	C1	50	25
	C2	25	50
	C3	25	125
5, 6 and 7	C1	60	25
	C2	25	60
	C3	25	125

Table 4. Layout of slab for multi-storey reinforced concrete building.

Number of storey	Slab type	Thickness (cm)	Description of slab
3, 4, 5, 6 and 7	S1	15	Slab carrying internal walls
	S2	15	Slab carrying internal walls
	S3	17	Slab for stairs
	S4	15	Slab for balcony

**Figure 4.** 3D View of structure by using STA4-CAD V12.1.**Table 5.** General building data.

Horizontal force factor (R,q)	7
Importance factor (I)	1
Live load participation factor (n)	0.3
Allowable bearing pressure*	20 t/m ²
Modulus of subgrade reaction*	2000 t/m ³
Concrete density	2.5 t/m ³
Earthquake analysis method	Mode superposition method
Seismic analysis min force load ratio (β)	0.9
Seismic loading eccentricity	0.12

*According to soil investigation report for Nicosia which have been done by geology and mines department of Northern Cyprus (Turkish Republic of Northern Cyprus, 2012).

Table 6. Specific building data according to EC8.

Seismic zone coefficient (a_{gR}) ¹	0.2
Spectrum characteristic period (T_b/T_c) ²	0.2/0.6
Design method	Eurocode ultimate design method

¹According to EC8 national annex of Cyprus for Nicosia region (CEN, 2004). ²According to soil investigation report for Nicosia which have been done by Geology and Mines department of Northern Cyprus (Turkish Republic of Northern Cyprus, 2012).

Table 7. Specific building data according to TEC2007.

Variable	Case I	Case II
Seismic zone coefficient (A_0)	0.2 ¹	0.3 ²
Spectrum characteristic period (T_a/T_b) ³	0.15/0.4	
Design method	TS-500 ultimate design method	

¹According to EC8 National Annex of Cyprus for Nicosia region (CEN, 2004). ²According to TEC2007 (Turkish Earthquake Code, 2007); ³According to soil investigation report for Nicosia which have been done by Geology and Mines department of Northern Cyprus (Turkish Republic of Northern Cyprus, 2012).

Table 8. Rough work unit price (2014).

Description	Unit	Unit Price(TL)
Reinforcements	Ton	2260
Concrete	m ³	148
Formwork	m ²	20

Specific data for reinforced concrete building design according to TEC2007

Turkey and Northern Cyprus are using TEC2007 recently. In this study, Case I and Case II are mentioned as follows:

Case I: data collected from the southern part of Cyprus which is considered as an official data, as shown in Table 6.

Case II: data collected from the northern part of Cyprus which is considered as a formal data used by civil engineers in Northern Cyprus, as shown in Table 7.

Upon the results of the analysis, quantity surveys of rough work constructions have been calculated with Northern Cyprus, Planning and Organization's office, 2014 unit prices praises, which is in Turkish-Lira (TL), as shown in Table 8 (Turkish Republic of Northern Cyprus, 2014). The bill of quantities presented did not include taxes or transportation fees.

RESULTS AND DISCUSSION

After the analysis and design of three to seven storey reinforced concrete buildings using STA4-CAD V12.1 computer program, according to EC8 and TEC2007, the total cost for super structures of an ordinary apartment buildings have been calculated and rough work cost per unit floor area is given in Figure 5.

As a result of the comparison of EC8 and TEC-2007 (Case II) as the number of storey increases, the difference of rough construction cost increases at the same time. TEC2007 provided higher ductility reduction factor compared to EC8. This has an effect on base shear.

The elastic response spectrum for acceleration, which is used for computing elastic earthquake force, shows diversity, from one earthquake to another and it is affected by local ground conditions. Theoretically, seismic ground motions are shown by elastic acceleration spectrum in both building codes. Spectrum characteristic periods are

defined due to the local site classes. The irregularities of analysis were examined in both regulations. For method of analysis, both similar static and dynamic procedures were used in EC8 and TEC-2007. During comparison, it has observed that there are only minor difference regarding calculation steps and limitations.

The design outputs of the program shows that the cross-sections for the structural elements are all same. The difference can be seen in the reinforcement amount. For a seven storey building located in Nicosia, for an ordinary apartment building data, according to TEC2007 (Case II), a percentage increase of 4.130 and 3.455% in steel reinforcement is observed compared to TEC2007 (Case I) and EC8 respectively.

The logical reason is that, the TEC-2007 lead us to be more precautionous with its own coefficients. According to European standards, looking from National annex of Cyprus, the seismic zonation map for Cyprus, Nicosia region, is assumed to be in the third earthquake region, in which, seismic zone coefficient, A_0 , is taken as 0.2. This condition is expressed as TEC-2007 (Case I). From this point of view, EC8 and TEC-2007 (Case I) show parallelism in terms of building cost.

Currently, there is no detailed and official seismic zone map announced by the government office. This results in high rough construction cost.

This paper only included the construction cost of the superstructure of the individual building system. Besides the individual structural system, other considerations should also be considered in the cost evaluation.

In the light of this study, Northern Cyprus has to specify its own official coefficients, suitable for its own conditions or the use of Eurocodes would be appropriate during the entry process of Northern Cyprus to European Union. Regarding the civil engineering perspective, it would be efficient to follow the improvements in the world.

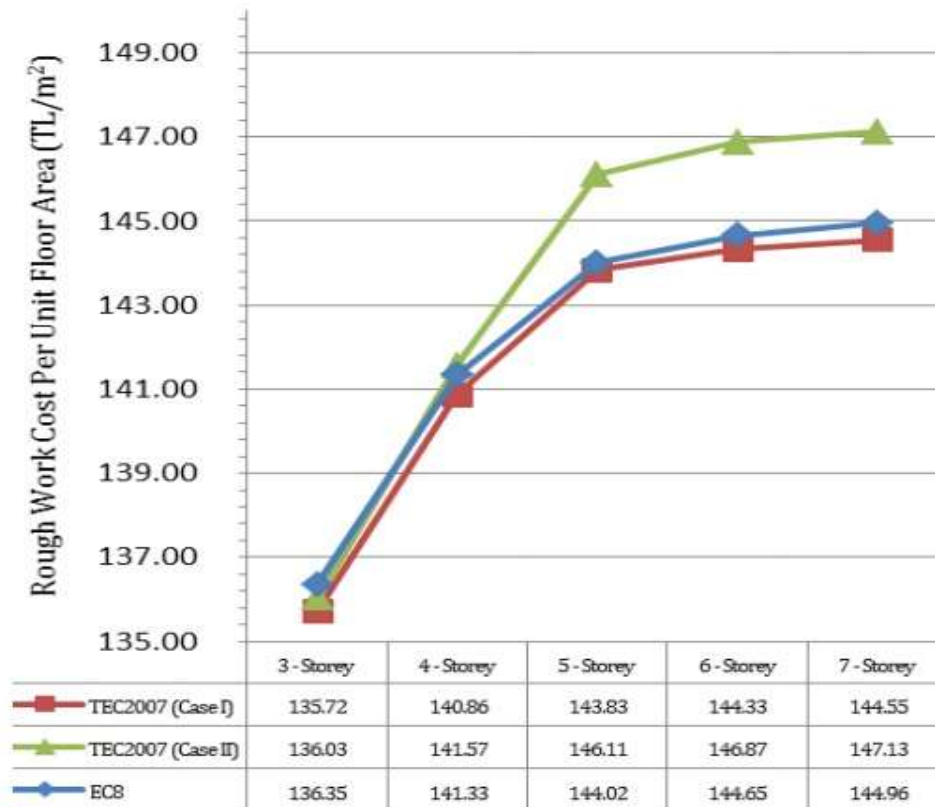


Figure 5. Rough work cost per unit floor area for an ordinary apartment building.

Conflict of Interests

The authors have not declared any conflict of interests.

REFERENCES

- Ambrasey N (2009). Earthquakes in the Mediterranean and Middle East: A Multidisciplinary Study of Seismicity up to 1900 (First ed.). Cambridge University Press.
- CEN (2004). Eurocode 2. Design of concrete structures - Part1: General rules for buildings, EN 1992-1:2004. Comite Europeen de Normalisation, Brussels.
- CEN (2004). Eurocode 8. Design of structures for earthquake resistance - Part1: General rules, seismic actions and rules for buildings, EN 1998-1:2004. Comite European de Normalisation, Brussels.
- Ersoy U, Ozcebe G, Tankut T (2000). Reinforced Concrete. Middle East Technical University, Department of Civil engineering. Turkey.
- Nunnally S (2007). Construction Methods and Management, Second Edition, Pearson. Prentice Hall, London.

Turkish Earthquake Code (2007). Ministry of Public Works and Settlement. Specification for Structures to be Built in Disaster Areas, Government of Republic of Turkey.

Turkish Republic of Northern Cyprus (2012). Ministry of Republic Works and Transport, Department of Metrology. Geological Office.

Turkish Republic of Northern Cyprus (2014). Planning and Organization's office.

Turkish Standards Institute (2000). TS-500, Requirements for design and construction of reinforced concrete structures, Ankara, Turkey.

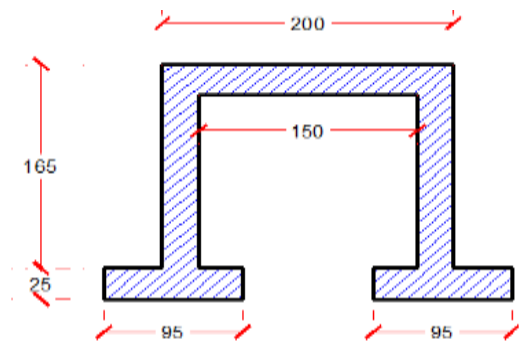
APPENDIX**Shear Wall Dimension Thick. = 25 Cm**
Dimension in Cm

Figure 1. Layout of shear-wall for multi-storey reinforced concrete buildings

Full Length Research Paper

Dynamic modelling and predictive health monitoring for vibration control and resonance of rotating machinery

A. Chellil^{1*}, I. Gahlouz^{2,3}, S. Lecheb¹, S. Chellil¹, A. Nour¹ and H. Mechakra¹

¹Dynamic of Engines and Vibroacoustic Laboratory, Industrial Maintenance Department, Université M'hamed Bougara de Boumerdes, Algeria.

²Industrial Maintenance Department, Université M'hamed Bougara de Boumerdes, Algeria.

³Poly Tech. Lille, LAGIS CNRS UMR 8219, 59655, Villeneuve d'Ascq Cedex, France.

Received 27 March, 2016 Accepted 27 September, 2016

The aim of this study is to investigate the critical speed analysis and response of a rotating machinery. The search for increasingly high performances in the field of the vibration phenomena which is subject rotor are increasingly important and can lead to system instability. The use of the finite element method makes to establish dynamic equations of the movement. Numerical calculations of the model developed, can extract the natural frequencies and modal deformed of the rotor, and this reduce is nonlinear. The Campbell diagram plot used to determine the critical speeds. Experimentally the study of the rotor in transient system allowed the determination of the spectral responses due to the unbalances and various excitations.

Key words: Stability, rotor, dynamic, critical speed.

INTRODUCTION

A detailed understanding of vibration problems associated with rotating systems is currently a major issue in the industrial field. To optimize the dynamic behavior of rotors and dimension to the best of such systems, Stodola (1972) worked out an iterative method to calculate the fundamental frequency of a vibrating system based on a standard form of eigen mode; it has been noted that the gyroscopic effect is a factor impacting the critical speed of a rotor. Si-Chaib et al. (2008) presented models based on the finite elements of flexible rotors to calculate the critical speeds and the eigen modes. In these models, the gyroscopic effects and the axial loadings are not taken into account. In the last few years, the most employed model has been

developed based on the finite element method (Nelson, 1980; Tran, 1981); which allowed the determination with good precision the eigen frequencies and the damping ratios, as well as the response to the various excitations. Moreover, this approach is modular because each element of the rotor is defined separately. Elements can thus be added or withdrawn according to the studied phenomena. The finite element method was thus used to study the embarked phenomena of damping in dynamics of the rotors (Duchemin, 2003). It was also applied to the study of the rotors whose shaft turns at variable speed (Al Majid, 2003). Many results concerning the dynamics of the rotors, whose support is fixed, have been reported for the models of Rayleigh-Ritz and the finite elements

*Corresponding author. E-mail: cchellil@yahoo.fr.

(Lalanne, 1998).

The experimental studies concerning the dynamics of the rotors are concentrated on inaccessible points by the theoretical way; these are the characteristics of bearing, dampings, actual stiffnesses, coefficients of sealing of the labyrinths and finally the flexibility of the foundations. Vance et al. (1987) compared the numerical and experimental results of the "free-free" modes and evaluate the precision of the model according to the coupling of the rotor with the discs. The Rayleigh-Ritz method is used to set up a model making it possible to treat simple cases and to highlight basic phenomena. A finite element model is developed to treat real systems. The equations of motion of the rotor are obtained by application of Lagrange equations.

The vibration indicators are used for fault detection and can track its evolution to manage the predictive maintenance

A fault diagnosis approach has been proposed by Wei et al., (2015) for rotating machines based on a new method for extracting and evaluating the statistical function; health condition is classified as the threshold corresponding is exceeded.

In this work, the dynamic behaviour of a rotor is discussed. The numerical study determines the deformed modes, evaluate Campbell's diagram and the response to the unbalance of the rotor in the vicinity of critical speeds.

The result for the estimation of the term vibration source on a particular line is shown in this paper, and the terms source estimated by both experimental and numerical methods are in excellent agreement with the theory.

Modelling of the rotors

The finite element method is very much used for the calculation of the complex structures is also efficient in dynamics of the rotors (Lalanne, 1998).

The elements of a rotor are: Disc, shaft and bearing. The kinetic energy T , the strain energy U and virtual work δW of external forces are calculated for all system elements to obtain the general equations of motion of a rotor.

It is necessary to define the finite elements making it possible modelling the rotors: discs, shaft, bearing and to represent external forces in particular those due to the unbalances.

The disc

The disk is assumed to be rigid. Only its kinetic energy is considered. The coordinate system x , y and z is connected to the coordinate system X , Y and Z through the angles ψ , θ and ϕ .

The angular velocity vector reflecting the position of the disc is written as:

$$\vec{\omega}_{R/R_0}^R = \begin{bmatrix} \omega_x \\ \omega_y \\ \omega_z \end{bmatrix} = \begin{bmatrix} -\dot{\psi} \cos \psi \sin \theta + \dot{\psi} \cos \theta \\ \dot{\theta} + \dot{\phi} \sin \psi \\ -\dot{\theta} \cos \theta \cos \psi + \dot{\theta} \sin \psi \end{bmatrix}_R \quad (1)$$

ω_x , ω_y and ω_z are the components of the angular velocity vector according to x , y and z . considering u and w coordinates of the center O of the disc along OX , OZ ; the following coordinated OY remaining constant.

The disk mass is m_d

The inertia tensor is noted:

$$I_{/o} = \begin{bmatrix} I_{dx} & 0 & 0 \\ 0 & I_{dy} & 0 \\ 0 & 0 & I_{dz} \end{bmatrix}_R \quad (2)$$

I_{dx} , I_{dy} and I_{dz} are the moments of inertia along the axis x , y and z respectively.

The general expression of the kinetic energy of the disc T_d is then written:

$$T_d = \frac{1}{2} m_d (\dot{u}^2 + \dot{w}^2) + \frac{1}{2} (I_{dx} \omega_x^2 + I_{dy} \omega_y^2 + I_{dz} \omega_z^2) \quad (3)$$

Or this expression can be simplified when the disc is symmetrical $I_{dx} = I_{dz}$. And when the angles θ and ψ are small and the angular velocity is constant, the Equation (3) becomes:

$$T_d = \frac{1}{2} m_d (\dot{u}^2 + \dot{w}^2) + \frac{1}{2} I_{dx} (\dot{\psi}^2 + \dot{\theta}^2) + \frac{1}{2} I_{dy} (\Omega^2 + 2\Omega \dot{\psi} \theta) \quad (4)$$

The term $\frac{1}{2} I_{dy} \Omega^2$, which is constant, has no influence on the equations of motion and represents the kinetic energy of the rotating disc at the rotational speed Ω , if all other displacement are zero. The last term $I_{dy} \Omega \dot{\psi} \theta$ is the gyroscopic effect (Coriolis).

The shaft

The shaft is assimilated to a beam of circular section and characterized by its kinetic and potential energies.

The expression of the kinetic energy is:

$$T_s = \frac{\rho S}{2} \int_0^L \left[\left(\frac{\partial u}{\partial t} \right)^2 + \left(\frac{\partial w}{\partial t} \right)^2 \right] dy + \frac{\rho I}{2} \int_0^L \left[\left(\frac{\partial \psi}{\partial t} \right)^2 + \left(\frac{\partial \theta}{\partial t} \right)^2 \right] dy + \rho I L \Omega^2 + 2\rho I \Omega \int_0^L \dot{\psi} \theta dy \quad (5)$$

ρ is the density, and S is the shaft section, I is the moment of inertia transverse (diametric).

The first integral of Equation 5 corresponds to the expression of the kinetic energy of a beam in bending, the second to the inertia effect due to the rotation and the last integral represents the gyroscopic effect.

The strain energy depends only on the stress and therefore the strain of the shaft relative to the support. In this calculation, one neglects the shear effects.

E is the Young modulus of the material, ε and σ represent respectively the strain and the stress, u^* and w^* are the displacements of the geometric center along the axes x and z (in the moving coordinate system).

The strain in bending of a point of the shaft with coordinate x and z in the reference frame R is

$$\varepsilon = \varepsilon_l + \varepsilon_{nl}$$

With the linear strain is given by:

$$\varepsilon_l = -x \frac{\partial^2 u^*}{\partial y^2} - z \frac{\partial^2 w^*}{\partial y^2} \tag{6}$$

The non linear strain is given by:

$$\varepsilon_{nl} = \frac{1}{2} \left(\frac{\partial u^*}{\partial y} \right)^2 + \frac{1}{2} \left(\frac{\partial w^*}{\partial y} \right)^2 \tag{7}$$

The general expression for the strain energy of the rotor in bending is then:

$$U = \frac{1}{2} \int_V \{\varepsilon\}^t [\sigma] d\tau \tag{8}$$

Where τ is the volume of the shaft and σ is the stress in bending.

The relationship between the stress and the strain is $\sigma = E\varepsilon$, are:

$$U = \frac{E}{2} \int_V (\varepsilon_l^2 + 2\varepsilon_l \varepsilon_{nl} + \varepsilon_{nl}^2) d\tau \tag{9}$$

Because of the symmetry of the shaft relative to the axes x and y , are obtained:

$$\int_V \varepsilon_{nl} \varepsilon_l d\tau = 0 \tag{10}$$

The third term of the integral (9) represents the effect of an axial force and is not considered in this study. Using the Equation 6 gives:

$$U = \frac{E}{2} \int_0^L \int_S \left(-x \frac{\partial^2 u^*}{\partial y^2} - z \frac{\partial^2 w^*}{\partial y^2} \right)^2 dS dy \tag{11}$$

$$U = \frac{E}{2} \int_0^L \int_S \left(x^2 \left(\frac{\partial^2 u^*}{\partial y^2} \right)^2 + z^2 \left(\frac{\partial^2 w^*}{\partial y^2} \right)^2 + 2xy \frac{\partial^2 u^*}{\partial y^2} \frac{\partial^2 w^*}{\partial y^2} \right) dS dy \tag{12}$$

By symmetry, the third term of Equation 12 is zero and, introducing the inertia of section:

$$\begin{aligned} I_x &= \int_S z^2 dS \\ I_z &= \int_S x^2 dS \\ \int_S xy dS &= 0 \end{aligned} \tag{13}$$

We find

$$U = \frac{E}{2} \int_0^L \left(I_z \left(\frac{\partial^2 u^*}{\partial y^2} \right)^2 + I_x \left(\frac{\partial^2 w^*}{\partial y^2} \right)^2 \right) dy \tag{14}$$

To avoid periodic terms, explicit function of time, it is necessary given considering the properties of bearings, to express the strain energy depending on u and w components of the displacement in the initial frame.

The passage of u^* , w^* at u , w is:

$$\begin{cases} u^* = u \cos \Omega t - w \sin \Omega t \\ w^* = u \sin \Omega t + w \cos \Omega t \end{cases} \tag{15}$$

Replacing u^* and w^* by their values (15):

$$U = \frac{E}{2} \int_0^L \left(I_z \left(\cos \Omega t \frac{\partial^2 u}{\partial y^2} - \sin \Omega t \frac{\partial^2 w}{\partial y^2} \right)^2 + I_x \left(\sin \Omega t \frac{\partial^2 u}{\partial y^2} + \cos \Omega t \frac{\partial^2 w}{\partial y^2} \right)^2 \right) dy \tag{16}$$

$$\begin{aligned} U &= \frac{E}{2} \int_0^L \left(\cos^2 \Omega t \left(\frac{\partial^2 u}{\partial y^2} \right)^2 + \sin^2 \Omega t \left(\frac{\partial^2 w}{\partial y^2} \right)^2 - 2 \frac{\partial^2 u}{\partial y^2} \frac{\partial^2 w}{\partial y^2} \cos \Omega t \sin \Omega t \right) \\ &+ I_x \left(\sin^2 \Omega t \left(\frac{\partial^2 u}{\partial y^2} \right)^2 + \cos^2 \Omega t \left(\frac{\partial^2 w}{\partial y^2} \right)^2 + 2 \frac{\partial^2 u}{\partial y^2} \frac{\partial^2 w}{\partial y^2} \cos \Omega t \sin \Omega t \right) dy \end{aligned} \tag{17}$$

For a symmetrical shaft, the expression of the strain energy becomes:

$$U = \frac{E}{2} \int_0^L I_z \left(\cos^2 \Omega t + \sin^2 \Omega t \right) \left(\frac{\partial^2 u}{\partial y^2} \right)^2 + (\sin^2 \Omega t + \cos^2 \Omega t) \left(\frac{\partial^2 w}{\partial y^2} \right)^2 dy \tag{18}$$

Finally:

$$U = \frac{E}{2} \int_0^L I_z \left(\left(\frac{\partial^2 u}{\partial y^2} \right)^2 + \left(\frac{\partial^2 w}{\partial y^2} \right)^2 \right) dy \tag{19}$$

Bearings

A bearing has the characteristics of stiffness and damping in the two planes. The forces applied by the bearings are due to displacement of the shaft relative to

the support.

The virtual work δW_p of external forces acting on the shaft of the first bearing is written as:

$$\begin{aligned} \delta W_p = & -k_{xx}u\delta u - k_{xz}w\delta u - k_{zx}u\delta w - k_{zz}w\delta w \\ & -c_{xx}\dot{u}\delta u - c_{xz}\dot{w}\delta u - c_{zx}\dot{u}\delta w - c_{zz}\dot{w}\delta w \end{aligned} \quad (20)$$

Similarly to the second bearing

Mass unbalance

The initial unbalance is generally distributed so as continuous on the rotor. The expression of the kinetic energy T_b of the unbalance is:

$$T_b = \frac{m_b}{2} (\dot{u}^2 + \dot{w}^2 + \Omega^2 d^2 + 2\Omega \dot{u} d \cos \Omega t - 2\Omega \dot{w} d \sin \Omega t) \quad (21)$$

m_b is the unbalance mass.

The term $\Omega^2 d^2/2$ is constant and will not intervene in the equations. The mass of the unbalance is negligible compared to the rotor mass; the expression of the kinetic energy can be approximated by:

$$T_b \approx m_b \Omega d (\dot{u} \cos \Omega t - \dot{w} \sin \Omega t) \quad (22)$$

The terms of the kinetic energy, strain energy and virtual work being established. The expressions of displacements in the X and Z directions are respectively set in the (separation of variables method):

$$\begin{aligned} u(y,t) &= f(y)q_1(t) = f(y)q_1 \\ w(y,t) &= f(y)q_2(t) = f(y)q_2 \end{aligned} \quad (23)$$

Where q_1 and q_2 are generalized independent coordinates.

The second order derivative of u and w displacements is necessary to express the elastic energy of the shaft:

$$\begin{aligned} \frac{\partial^2 u}{\partial y^2} &= \frac{d^2 f(y)}{dy^2} q_1 = h(y)q_1 \\ \frac{\partial^2 w}{\partial y^2} &= \frac{d^2 f(y)}{dy^2} q_2 = h(y)q_2 \end{aligned} \quad (24)$$

The functions $g(y)$ and $h(y)$ represents the first derivative and the second derivative respectively. Given that the angular displacements, ψ and θ are small, they are approached by:

$$\begin{cases} \theta = \frac{\partial w}{\partial y} = \frac{df(y)}{dy} q_2 = g(y)q_2 \\ \psi = -\frac{\partial u}{\partial y} = -\frac{df(y)}{dy} q_1 = -g(y)q_1 \end{cases} \quad (25)$$

The displacement function f is chosen to represent exactly the form of the first mode of a constant section beam in bending on two simply supported situated at its ends.

$$f(y) = \sin \frac{\pi y}{L} \quad (26)$$

Hence,

$$g(y) = \frac{\pi}{L} \cos \frac{\pi y}{L} \quad (27)$$

$$h(y) = -\left(\frac{\pi}{L}\right)^2 \sin \frac{\pi y}{L} \quad (28)$$

Substituting in the expressions of (25) where (4), we find: The kinetic energy of the disk T_D can be written as follows:

$$\begin{aligned} T_D = \frac{1}{2} \left[M_D f^2(y_{disk}) + I_{Dx} g^2(y_{disk}) \right] (\dot{q}_1^2 + \dot{q}_2^2) \\ - I_{Dy} \Omega g^2(y_{disk}) \dot{q}_1 \dot{q}_2 \end{aligned} \quad (29)$$

The expression for the kinetic energy of the shaft T_s is:

$$\begin{aligned} T_s = \frac{1}{2} \left[\rho S \int_0^L f^2(y) dy + \rho I \int_0^L g^2(y) dy \right] (\dot{q}_1^2 + \dot{q}_2^2) \\ - 2\rho I \Omega \int_0^L g^2(y) dy \dot{q}_1 \dot{q}_2 \end{aligned} \quad (30)$$

The strain energy of the shaft is:

$$U_s = \frac{EI}{2} \int_0^L h^2(y) dy (q_1^2 + q_2^2) \quad (31)$$

The kinetic energy of the ensemble disk - rotor is given by:

$$\begin{aligned} T_{DS} = T_s + T_D = \left[\frac{1}{2} (M_D f^2(y_{disk}) + I_{Dx} g^2(y_{disk})) \right. \\ \left. + \frac{1}{2} \left(\rho S \int_0^L f^2(y) dy + \rho I \int_0^L g^2(y) dy \right) \right] (\dot{q}_1^2 + \dot{q}_2^2) \\ - I_{Dy} g^2(y_{disk}) + 2\rho I \int_0^L g^2(y) dy \Omega \dot{q}_1 \dot{q}_2 \end{aligned} \quad (32)$$

The kinetic energy of the unbalance is:

$$T_u = m_b d \Omega f(y_{bal}) (\dot{q}_1 \cos \Omega t - \dot{q}_2 \sin \Omega t) \quad (33)$$

Where T_d, T_a, T_b are the respective kinetic energies of the

disc, shaft, of the unbalance.

The application of Lagrange equations:

$$\frac{d}{dt} \left(\frac{\partial T_c}{\partial \dot{q}_i} \right) - \frac{\partial T_c}{\partial q_i} + \frac{\partial U}{\partial q_i} = \delta W_i \quad (34)$$

avec $i=1, 2$.

Which in general form are written:

$$\begin{aligned} & \left[M_D f^2(y_{disk}) + I_{Dx} g^2(y_{disk}) + \rho S \int_0^L f^2(y) dy + \rho I \int_0^L g^2(y) dy \right] \ddot{q}_1 \\ & - \left[I_{Dy} g^2(y_{disk}) + 2\rho I \int_0^L g^2(y) dy \right] \Omega \dot{q}_2 + k q_1 = m_b d \Omega^2 f(l_1) \sin \Omega t \quad (35) \\ & \left[M_D f^2(y_{disk}) + I_{Dx} g^2(y_{disk}) + \rho S \int_0^L f^2(y) dy + \rho I \int_0^L g^2(y) dy \right] \ddot{q}_2 \\ & + \left[I_{Dy} g^2(y_{disk}) + 2\rho I \int_0^L g^2(y) dy \right] \Omega \dot{q}_1 + k q_2 = m_b d \Omega^2 f(l_1) \cos \Omega t \end{aligned}$$

Solving this system of equations provides the expressions of frequencies and deflections of the tree line in each of its points.

Modal analysis and numerical simulation

It is about the calculation of the dynamic behaviour of a rotor step by step in time. The objective is to present a model of calculation using a simplified approach. The construction of the grid is made with ANSYS software starting from the characteristics of the various elements of the rotor. Modelling by finite elements requires the supply of data relating to the geometry (coordinated nodes), boundary conditions, and description of the elements (disc, bearing, and additional elements) of mechanical characteristics of materials and bearing, function of the rotation speed and on the information relative to the excitations.

The finite element Model of the rotor is carried out with the code ANSYS. The shaft is discredited by the beam element to 4 degrees of freedom by node: two displacements U and W and two rotations according to Y and Z. The disc is supposed to be rigid. This model makes it possible to carry out temporal simulations of the dynamic behaviour of the rotor.

The disc is assumed to be perfectly rigid and it's modeling using a pipe element (Pipe16). To model the shaft using the beam element (Beam189). For modeling the bearings are used spring-damper element (Combin14).

The finite element model of the rotor consists of a shaft, disc and bearings. The length and outer diameter of the shaft is $L=1.4 \text{ m}$ $r = 0.15 \text{ m}$ respectively. The inner diameter and outer diameter of the disc is $r_1 = 0.15 \text{ m}$ and $r_2 = 0.625 \text{ m}$ respectively.

The material is a special steel assumed homogeneous and isotropic, with density $\rho_d = 7850 \text{ kg/m}^3$, Poisson's ratio $\nu = 0.3$ and elastic Young's modulus $E_a = 248 \text{ GPa}$.

The disc is a special steel assumed to be homogeneous, isotropic and having $\rho_d = 7850 \text{ kg/m}^3$, Poisson's ratio $\nu = 0.3$ and elastic Young's modulus $E_a = 248 \text{ GPa}$.

The stiffness and the damping for the first bearing is:

$$k_{yy} = 1.10^8 \text{ N/m}, \quad k_{zz} = 8.10^7 \text{ N/m},$$

$$c_{yy} = 1.2.10^4 \text{ N.s/m}, \quad c_{zz} = 8.10^3 \text{ N.s/m}$$

The stiffness and the damping for the second bearing is:

$$k_{yy} = 7.10^8 \text{ N/m}, \quad k_{zz} = 5.10^7 \text{ N/m},$$

$$c_{yy} = 8.10^3 \text{ N.s/m}, \quad c_{zz} = 6.10^3 \text{ N.s/m}$$

The calculation is made from the discretization of the shaft into several elements, once the data is entered the geometric model is established and it resulted in the rotor mesh (Figure 1). All numerical data on the mesh of the rotor is summarized in Table 1. The model comprises 51 nodes, or 204° of freedom and ale modal base consists of five modes.

Boundary conditions

The characterization of the rotor can be made by its decomposition into flexible finite element and therefore study node by node boundary conditions.

During the movement, the center line of the shaft does not remain confused with the original right are (Ux, Uy, Uz) displacements of the shaft, Uy and Uz are variables while Ux is considered as constant since only the shaft deflection movements are studied.

So for the nodes of the two bearings we annul all degrees of freedom, for the nodes of the rotor we annul the degrees of freedom of translation and rotation along the x axis (Figure 2), there are only four degrees of freedom per node, two rotations according y and z, and two translations according y and z.

Evolution of the stress

A force is applied on the disc, and thereafter determines the equivalent Von Mises stress in static analysis (Figure 3). The concentration of stress is observed at the connection between the shaft and the disc. The maximal stress is 201 Mpa; this is a sensitive area for the appearance of defects.

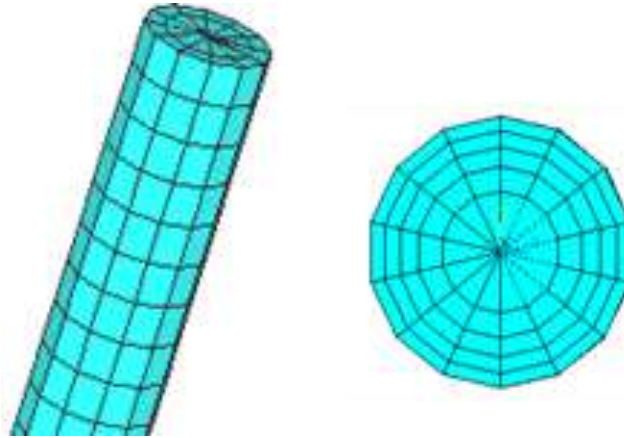


Figure 1. Rotor meshing.

Table 1. the number of element, nodes and degrees of freedom of the rotor.

Structure	Element	Nodes	Degrees of freedom
Rotor	30	51	204

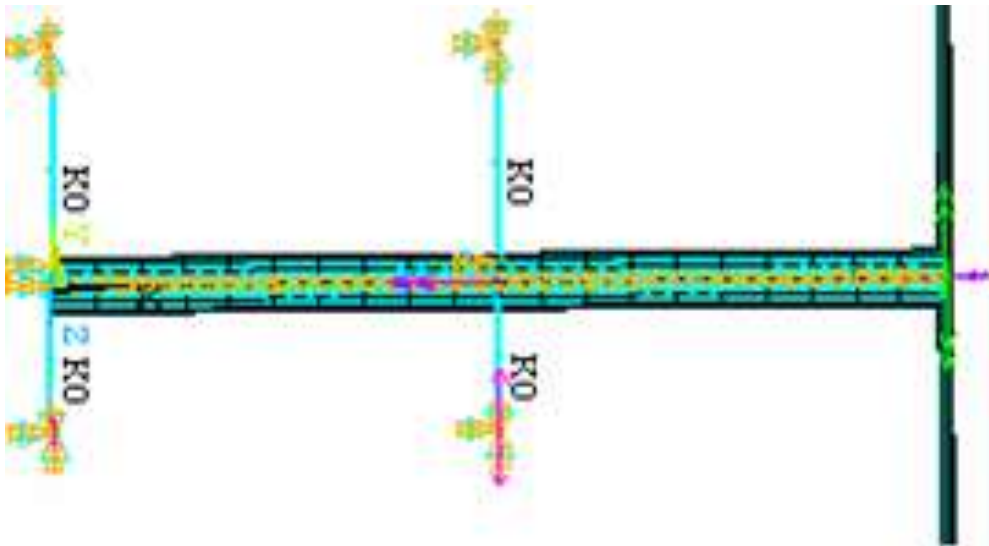


Figure 2. Boundary conditions of the rotor.

Modal analysis

The modal base consists of five modes. The objective of this study is to determine the eigen frequencies and eigen modes and the stresses of bending vibration of the rotor. The eigen frequencies are represented on the Table 2.

The modal base contains five modes. The allure of the three modes of the rotor and their orbits of mode shapes

at any rotational speed is shown in Figures 4 to 6. These modes are characterized by local bending.

Campbell diagram

The critical speeds are given by the intersection points of the excitation sources (Harmonics 1, 4, 5 ...) with the natural modes to direct precession and reverse precession.

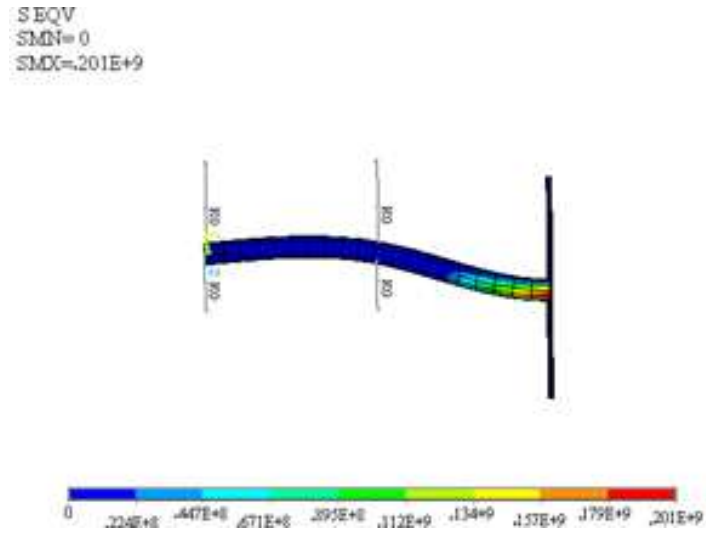


Figure 3. Evolution of the Von Mises equivalent stress.

Table 2. Eigen frequencies of the rotor.

Mode	1	2	3	4	5
Frequency (Hz)	27	42	120	220	310

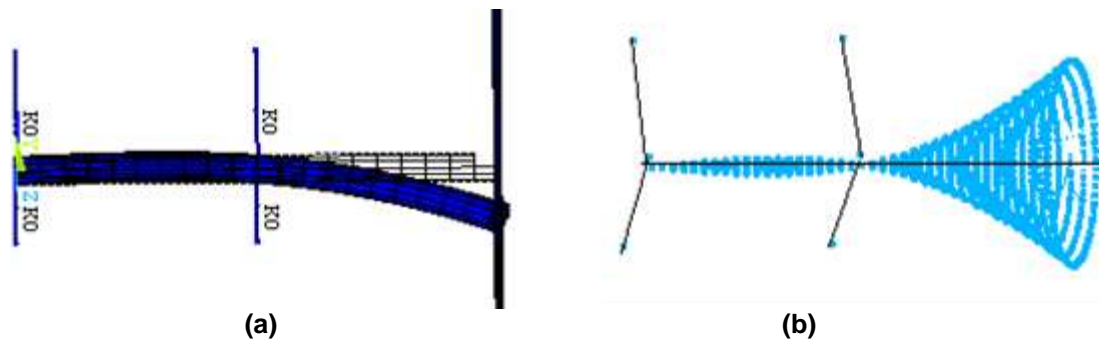


Figure 4. The first mode (a) The first mode shapes ($f=27\text{Hz}$, $D_{\text{max}}=0.0051$); (b) The orbits of mode shapes at 258 rpm.

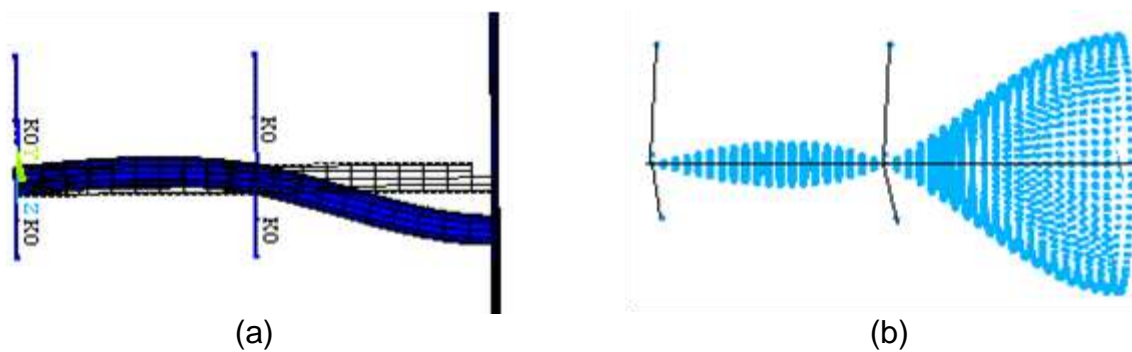


Figure 5. The third mode (a) The third mode shapes ($f=120\text{ Hz}$, $D_{\text{max}}=0.0062$); (b) The orbits of mode shapes at 1146.5 rpm.

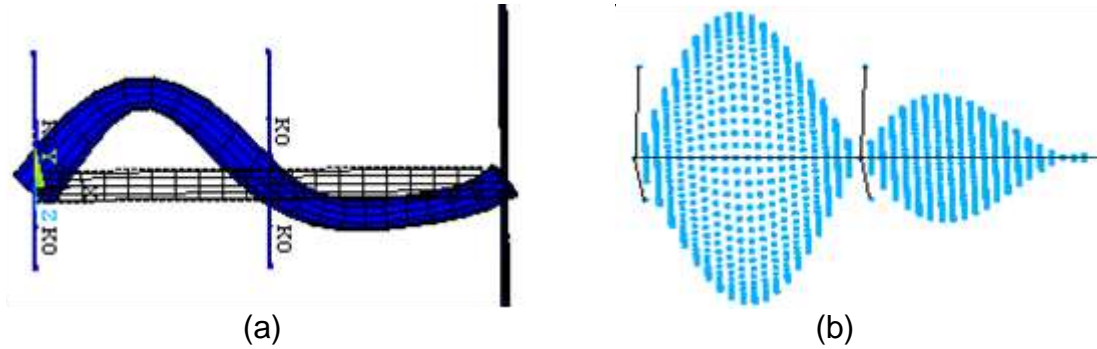


Figure 6. The five mode (a) The five mode shapes ($f = 310$ Hz, $D_{max} = 0.042$); (b) The orbits of mode shapes at 2262 rpm.

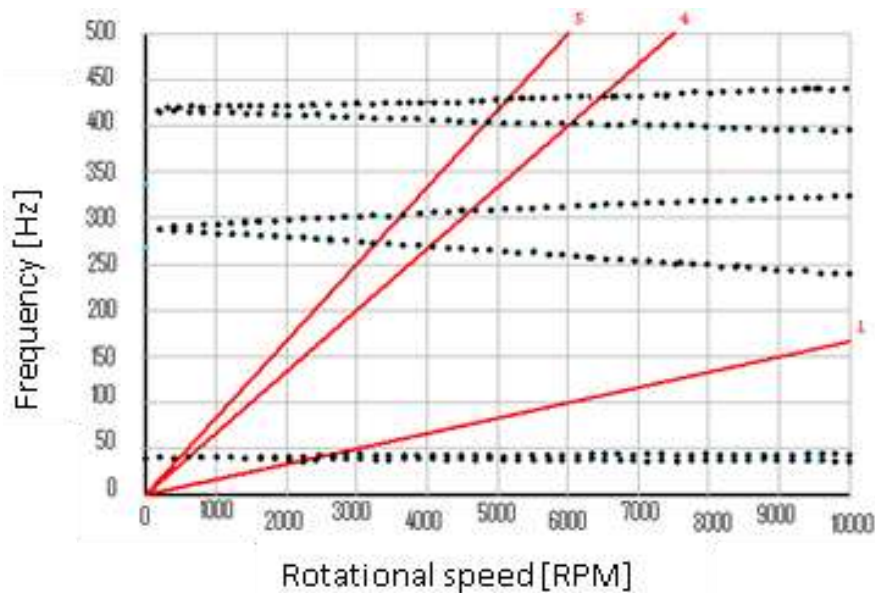


Figure 7. The diagram of Campbell.

We get Campbell diagram (Lalanne, 1998; Genta, 1992; Muszynska, 1996; Mogenier, 2012; Saad and Seamus, 2011).

The diagram of Campbell (Figure 7) shows that the first critical speeds (for the harmonic in the order 1, 4 and 5). For the harmonic of order 1, which corresponds to the first mode of the shaft at the speed of 2500 rev/min (40 Hz)? For the harmonic of order 4, the first critical speed is 600 rev/min (40 Hz); the second critical speed is 4000 rev/min (270Hz) and finally 4500 rev/min (310 Hz).

Spectrum of frequency response

The results in the Fourier spectrum Figure 8 are obtained from the numerical simulation. The rotor is subject to an unbalance of 0001 kg and an asynchronous force with

the intensity is 1 N placed at node number 19 for $L = 1.4$ m, for a rotational speed equal to 500 rpm. After running, the responses of each node is obtained, the results of the responses at the node Number 19 are presented as graphs showing the spectral response.

Figure 8 represents the frequency response curve for speeds of rotation from 0 to 500 RPM .The frequency at which the peak response occurs 18 and 37 Hz is. The first frequency is explained by an initial shock due to the applied force. The second frequency corresponds to the frequency of the critical speed of the associated linear system, it amounts to the initial unbalance.

MATERIALS AND METHODS

Vibration monitoring generally used to monitor in real time and without interruption the vibration behavior of rotating machines. A

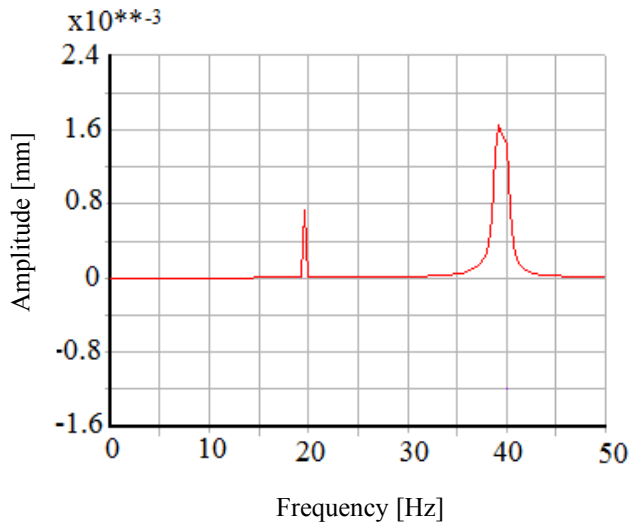


Figure 8. Spectrum of frequency response.

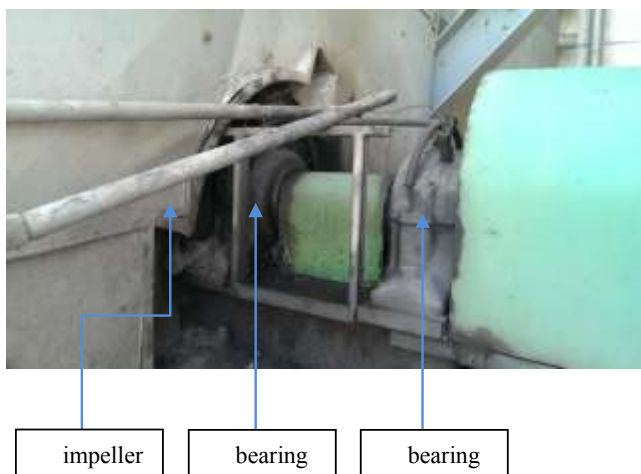


Figure 9. The combustion air ventilator components.

wide variety of techniques have been used for fault detection and diagnosis in rotating machinery. These techniques can be classified into frequency domain, time domain, time-frequency domain and other and techniques (Kumar et al., 2013; Kumar and Kumar, 2014; Jalan and Mohanty, 2009; Yang and Court, 2009; Chellil et al., 2015). This study will primarily investigate techniques based on the time domain, frequency domain and time-frequency domain [Ding et al., 2016] detailed spectral analysis is presented by Yamamoto et al. (2016), the results clearly show the feasibility of this experimental intelligent diagnostic approach for measuring vibration and unbalance fault detection in rotating machinery.

A case of industrial survey was treated for validate the approach and to show that in some cases exceeding the thresholds imposed by the standards represent a defect synonymous. We will make the establishment of the rotor vibration analysis following the method of OFF LINE system. The measurements are performed at regular time intervals (periodically) by portable systems increasingly informatics. The aim of this work is to do a vibration analysis (monitoring and diagnostic) to study vibration phenomena emerged

the rotor.

The combustion air ventilators have the task of feeding the steam generator combustion area required in power plants. They aspire outside air and do to the burners through air preheater. In this case the ventilator is composed of a shaft, impeller and two bearings (Figure 9). The high quality steel shaft, the impeller is high quality steel; it is mounted on a cylindrical seat on the shaft by means of an interference fit oil seal. The shaft is mounted in two bearings at bearings type FAG SN 328 and FAG 22328 ES.

Equipments used for test

The measurements were realized using the following equipment.

Vibration sensor

This is an AS-065 piezoelectric accelerometer connected to the VIBROTEST 60 analyzer manifold. This sensor is used to measure vibration acceleration (Figure 10b).

Vibrotest 60 analyzer

The VIBROTEST 60 (Figure 10c) is a practical acquisition apparatus for making: global vibration measurements, process parameter, time signals and spectral signals.

The implementation of the accelerometer on the machines is very important. Each measurement companion must be performed at specific points and always the same. We try to close as possible points of measurements of bearings; it allowed us to get the most loyal mechanical defects images.

RESULTS AND DISCUSSION

Figure 11a and b represent the measurements of vibrations in the horizontal direction (Bearing 1) and the vertical direction (Bearing 2) of the pump.

The first spectral line in the first spectrum (Figure 4a) has an amplitude of 0.47 mm/s, this value exceeds the warning threshold, the frequency of this line is 9.88 Hz (95 rev / min), the speed is the rotational speed of the rotor.

The 2nd spectral line in the same spectrum (Figure 4a) has amplitude of 0.9 mm/s and a frequency 153.76 Hz. This value is below the alert threshold and not a danger.

The first spectral line in the first spectrum (Figure 4b) has an amplitude of 0.235 mm/s when it exceeds the threshold. The frequency of this line is 50 Hz (477.70 rev / min), the speed is the speed of rotation of the rotor.

The 2nd spectral line in the same spectrum (Figure 4b) has an amplitude of 0.14 mm/s and a frequency 153.76 Hz. This value is below the alert value and is not dangerous.

The 1st two spectral lines on the two spectra (Figure 4a and b) are on the same frequency of rotation of the shaft and we have high vibration speed on the three directions of measurements, so this symptom tells us about the existence of a defect unbalance.

The two spectral lines that follow have frequencies equal to twice the rotation frequency of the shaft, the



(a)



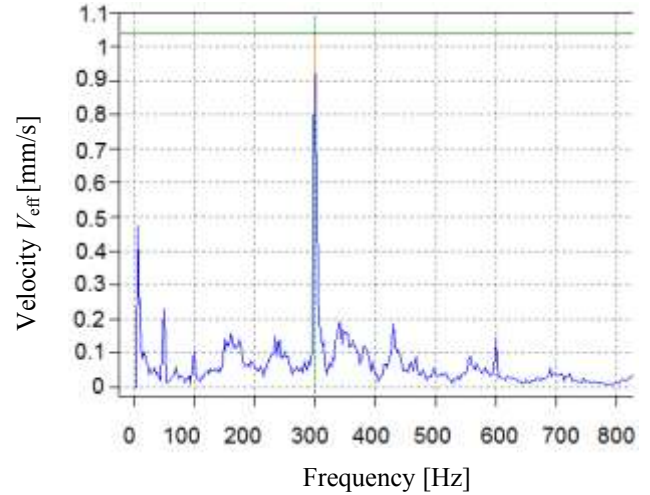
(b)



(c)

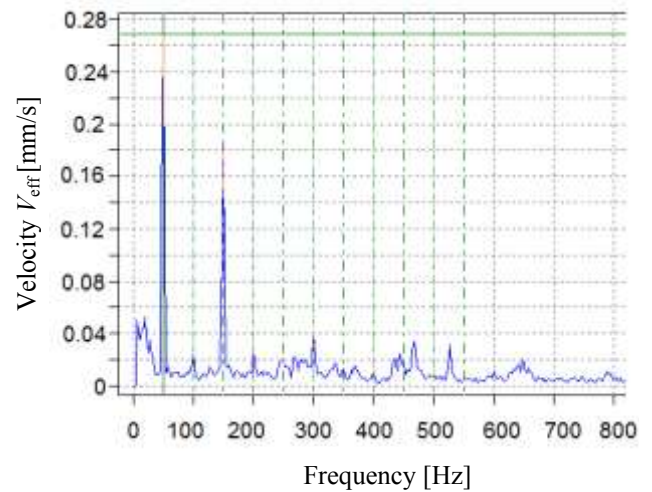
Figure 10. Equipments used for test (a) Equipments used for test measurement of vibration; (b) Accelerometer AS-065; (c) Vibrotest 60.

◆ Signal of Bearing 1 (Horizontal direction)



(a)

◆ Signal of Bearing 2 (Vertical direction)



(b)

Figure 11. Spectral responses of the bearings (a) Horizontal bearing1 spectrum; (b) Vertical bearing 2 spectrums.

amplitude of the vibration levels are below the warning threshold, they are due to the significance of this imbalance in the two bearings of the pump shaft. Once the fault is repaired the vibration must disappear.

Conclusion

The model of finite elements of the rotor was designed starting from a well defined geometry. An effective interpretation of the frequencies and modal deformations

of the model were simulated. The distribution of the stress along the rotor was identified. In the present case, the maximum stress is 201 Mpa were concentrated at the connection between the shaft and the disc. The differences on the level of the maximum amplitude of the vibrations can be easily reduced significantly with the geometrical model. Nevertheless, as the critical speed depends on the considered shape, one can determine the intensity of the amplitude on the response curve to unbalance. The layout of the response to an unbalance presents brutal increases in the amplitude of vibration of the rotor. In this article, an detection system based on industrial signals treated in the frequency domain is proposed. The results were presented to identify and detect unbalanced faults in bearing. The analysis of measurement results shows the presence of an unbalance fault on the rotating machinery. This defect is the cause of a long shutdown and poor conditions present during shutdown, it is recommended to remedy a bearing balancing the rotating machinery.

Conflict of Interests

The authors have not declared any conflict of interests.

REFERENCES

- Al Majid A, Allezy A, Dufour R (2003). Metric of MDOF systems in high transient motion, Proceedings of ASIVIE Design Engineering Technical Conferences, 2-6 September. Chicago. USA. P 6.
- Chellil A (2015). Condition Monitoring for Controlling the Stability of the Rotating Machinery. *Int. J. Mech. Aerosp. Ind. Mech. Man. Eng.* 9(12):2030-2035.
- Ding Y, He W, Chen B, Zi Y, Selesnick IW (2016). Detection of faults in rotating machinery using periodic time-frequency sparsity. *J. Sound Vib.* 382:357-378.
- Duchemin M (2003). Contribution à l'étude du comportement dynamique d'un rotor embarqué. Thèse de doctorat de l'INSA-Lyon.
- Genta G (1992). A fast modal technique for the computation of the Campbell diagram of multi-degree-of-freedom rotors". *J. Sound Vib.* 155(3):385-402.
- Jalan AK, Mohanty AR (2009). Model based fault diagnosis of a rotor bearing system for misalignment and unbalance under steady state condition. *J. Sound Vib.* 327:604-622.
- Kumar PS, Abraham A, Bensingh RJ, Ilangoan S (2013). Computational and Experimental analysis of a Counter-Rotating Wind Turbine system. *J. Sci. Ind. Res.* 72(05):300-306.
- Kumar SS, Kumar MS (2014). Condition Monitoring of rotating machinery through Vibration Analysis. *J. Sci. Ind. Res.* 73(04):258-261.
- Lalanne M, Ferraris G (1998). Rotordynamics prediction in engineering. 2nd Edition. Chichester, John Wiley. P 254.
- Mogenier G, Baranger T, Ferraris G, Dufour R, Durantay L (2012). The problem of complex shape tracking in a Campbell Diagram or how to overcome crossing/veering phenomena. 10th International Conference on Vibrations in Rotating Machinery. pp. 257-267.
- Muszynska A (1996). Forward and backward precession of a vertical anisotropically supported rotor. *J. Sound Vib.* 192(1):207-222.
- Nelson HD (1980). A Finite Rotating Shaft Element Using Timoshenko Beam Theory. *J. Mech. Des. Trans. ASME* 102:793-803.
- Saad SA, Seamus DG (2011). Modal correlation approaches for general second-order systems: Matching mode pairs and an application to Campbell diagrams. *J. Sound Vib.* 330(23):5615-5627.
- Si-Chaib M, Chellil A, Nour A, Saci R, Chikh N, Chevalier Y (2008). Numerical and experimental investigation of the dynamic behavior a vertical rotor. 15th International Congress on Sound and Vibration. Daejeon. Korea. Proceed. ICSV 15:2347-2354.
- Stodola A (1927). Steam and Gas Turbines. McGraw-Hill. New York. Vol. I.
- Tran DM (1981). Etude du comportement dynamique des rotors flexibles. Thèse Université C. Bernard. Lyon.
- Vance JM, Murphy BT, Tripp HA (1987). Critical speeds of turbo machinery; computer predictions versus experimental measurements. *J. Vib. Acoust.* 109:1-7.
- Wei L, Zhencai Z, Fan J, Gongbo Z, Guoan C (2015). Fault diagnosis of rotating machinery with a novel statistical feature extraction and evaluation method. *Mech. Syst. Signal Process.* 50(51):414-426.
- Yamamoto GK, da Costa C, da Silva Sousa JS (2016). A smart experimental setup for vibration measurement and imbalance fault detection in rotating machinery. *Case Stud. Mech. Syst. Signal Process.* 4:8-18.
- Yang W, Court R (2013). Experimental study on the optimum time for conducting bearing maintenance. *Measurement* 46:2781-2791.

Scientific Research and Essays

Related Journals Published by Academic Journals

- African Journal of Mathematics and Computer Science Research
- International Journal of Physical Sciences
- Journal of Oceanography and Marine Science
- International Journal of Peace and Development Studies
- International NGO Journal

academicJournals